A generic framework for reliability assessment of offshore wind turbine monopiles considering soil-solid interaction and harsh marine environments

Lin Wang & Athanasios Kolios
Centre for Offshore Renewable Energy Engineering, School of Water, Energy and Environment, Cranfield University, Cranfield, MK43 0AL, UK

ABSTRACT: OWT (offshore wind turbine) monopiles may experience significant soil-solid interactions and are exposed to harsh marine environments with great uncertainty (e.g. soil properties, wind, wave and current loads, etc.), making their reliability assessment quite challenging. In this work, a generic framework for reliability assessment of OWT monopiles is developed. The framework starts with defining limit states, which distinguish a failure and a safe region of operation. Four types of limit states are considered, i.e. ultimate, fatigue, deflection and buckling limit states. The uncertainties in wind, wave and current loads as well as soil properties are taken into account by modelling them stochastically. A 3D (three-dimensional) parametric FEA (finite element analysis) model of OWT monopiles is developed, taking account of soil-solid interaction and stochastic variables (i.e. soil properties, wind, wave and current loads). Multivariate regression is used to post-process the results of stochastic FEA simulations to derive limit-state performance functions expressed in terms of stochastic variables. Having obtained the performance functions, the FORM (first order reliability method) is then used to calculate the reliability index for each limit state, evaluating the reliability of OWT monopiles. The proposed framework is applied to a 30m-length OWT monopile to assess its reliability. The results indicate that the fatigue reliability is dominant in the design of OWT monopiles. The proposed framework is generic and capable of effectively assessing reliability of OWT monopiles, providing the possibility to optimise the OWT monopiles to meet target reliability.

1 INTROUCTION

Over the past 15 years, wind power technology has experienced significant development with over 1500% increase in global annual wind power installation, reaching a total installed capacity of 432 GW at the end of 2015 (Council, 2016). Giving the continuous increasing trend of rotor size (Wang et al., 2016b), and since OWTs (offshore wind turbines) make benefit of larger available space, it is observed that an increasing part of R&D investments are allocated to OWTs (EWEA, 2016). Offshore wind has officially become the most profitable renewable energy source due to the huge development it experienced in Europe. According to European Wind Energy Association (EWEA, 2015), offshore wind in Europe will reach 64.8 GW, supplying 8.4% of total electricity demand in Europe in 2030.

Due to their ease of both fabrication and installation, monopiles are currently the most commonly used foundation for OWTs, representing 80.1% of total EU's installation in 2015 (Wilkes et al., 2016). They are well suitable for water depths ranging from 5m to 30m.

OWT monopiles may experience significant soil-solid interactions and are exposed to harsh marine environments with great uncertainty (e.g. soil properties, wind, wave and current loads, etc.), making their reliability assessment quite challenging. The reliability assessment of OWT monopiles requires a structural model of monopiles to determine the structural responses of the monopile structures subjected to both soil-solid interaction and loads induced by harsh marine environments. Appropriate reliability methods, e.g. FORM (First Order Reliabiltiy Method) should be employed in order to evaluate the probability of failure.

Structural models used for OWT monopiles can be roughly categorised into two groups, i.e. 1) 1D (one-dimensional) beam model, in which monopile structures are discretised into a series of beam elements; and 2) 3D (three-dimensional) FEA (finite element analysis) model, in which monopile structures are constructed using shell or brick elements. The 1D beam model is computationally efficient and capable of providing reasonable results to model global structural behaviour, such as deflections and modal frequencies (Wang et al., 2014). However, it fails to represent accurately

structural responses at local scale, such as stress concentration effects (Petrini et al., 2010). In order to capture structural responses accurately, it is necessary to construct the monopile structures using 3D FEA. Compared to the 1D beam model, the 3D FEA model is capable of examining detailed stress distributions within the structure and capturing structural responses accurately. Due to its high fidelity, the 3D FEA model has been widely applied to model wind turbine structures (Wang et al., 2016c, Wang et al., 2015, Abdel-Rahman and Achmus, 2005, Wang et al., 2016a). Therefore, 3D FEA model is chosen in this study to determine the structural responses of OWT monopiles.

Due to the fact that part of a OWT monopile (i.e. monopile foundation) is embedded into the soil, the soil-structure interaction should be considered in order to accurately capture the structural responses of OWT monopiles. A simple way to model the soil is the p-y method (SM, 2000), in which the soil is modelled by equivalent springs with stiffness based on soil properties. However, this method was developed and valid for the Oil and Gas industry only, which is not suitable for larger pile diameters used for OWT monopiles. Consequently, the p-y method tends to overestimate the pile-soil stiffness and underestimate lateral deflections (Jung et al., 2015). A recommended way to obtain accurate and reliable results is to use 3D FEA with brick elements to model the soil (GL, 2016, Jung et al., 2015). Considering the accuracy, the 3D FEA with brick elements is chosen in this study to model the soil.

This paper attempts to develop a generic framework for reliability assessment of OWT monopiles, considering soil-solid interaction and harsh marine environments. A 3D parametric FEA model of OWT monopiles is developed, taking account of soil-soild interaction and stochastic variables. Multivariate regression is used to post-process the results of stochastic FEA simulations to obtain limit-state performance functions expressed in terms of stochastic variables. After that, the FORM is used to calculate the reliability index for each limit state. The proposed framework is applied to a 30m-length OWT monopile to assess its reliability.

This paper is structured as follows. Section 2 presents the parametric FEA model. Section 3 presents the implementation of structural reliability assessment. Section 4 presents the results and discussion, followed by conclusions in Section 5.

2 PARAMETRIC FEA MODEL

A parametric FEA model of OWT monopiles is developed using ANSYS, which is a widely used commercial FE software. The parametric FEA model enables the stochastic modelling of OWT monopiles with stochastic variables (such as loads and material properties). The geometry, materials, mesh, loads and boundary conditions used in the parametric FEA model are presented below.

2.1 *Geometry*

The monopile used in this study has an outer diameter of 5m and an overall length of 30m, consisting of ten 3m-length segments with varied thickness (see Fig. 1a). The soil is modelled as a cylindrical body with a depth of 30m and a diameter of 75m. The depth of soil is divided into three layers, i.e. loose sand, medium clay and medium sand. 15m of the monopile is embedded into the soil, and the remaining 15m covers the distance from the seabed level up to the sea surface. Figure 1 depicts the geometry model.

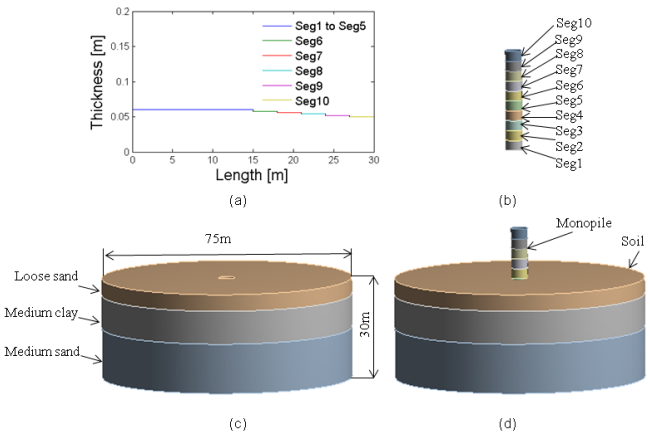

Figure 1. Geometry: **a** thickness distributions of monopile, **b** monopile, **c** soil, **d** assembly

2.2 *Materials*

2.2.1 *Monopile material*

The monopile is made of S355 structural steel, which is a widely used material for OWT support structures. This material has isotropic elastic behaviour, and its properties are listed in Table 1.

Table 1. Properties of S355 structural steel (GL, 2016)

Property	Value
Density [kg/m^3]	7800
Young's modulus [GPa]	210
Poisson's ratio [-]	0.28
Yield strength [MPa]	355

2.2.2 *Soil profile*

Three types of soil (i.e. loose sand, medium clay and medium sand) are assigned with the Drucker-Prager Strength Linear model (Drucker and Prager, 1952) which has been widely used to represent the behaviour of soils. In this model, the cohesion and compaction behaviour of the materials result in an in-

creasing resistance to shear up to a limiting value of yield strength as the loading increases. The yield strength of these materials is highly dependent on pressure, and the yield stress is taken as a linear function of pressure. According to Drucker-Prager model, the yield strength of the soil, $\sigma_{y,s}$, can be expressed in terms of cohesion coefficient c and friction angle ϕ using the following equation:

$$\sigma_{y,s} = \frac{6c\cos(\phi)}{\sqrt{3}(3-\sin(\phi))} \quad (1)$$

Table 2 summarises the properties of the soil model used in this study.

Table 2. Summary of properties of the soil model (Brady and Weil, 1996, Geotechdata, 2016)

Item	Vaules		
	Layer 1	Layer 2	Layer 3
Type of soil	Loose sand	Medium clay	Medium sand
Depth [m]	0-5	5-15	15-30
Density [kg/m^3]	1850	1910	1975
Young's modulus [MPa]	24	50	53
Poisson's ratio	0.3	0.3	0.3
Cohesion coefficient [kPa]	50	15	63
Friction angle [deg.]	29.5	23	33.0
Yield stress [kPa]	60.1	18.3	74.5

2.3 *Mesh*

The monopile is a thin-walled structure, and therefore shell elements can be used to model it accurately and efficiently. This is not the case for the soil layers, and therefore the soil is modelled using brick elements. For both monopile and soil, a regular mesh generation method is used to generate high quality elements, ensuring computational accuracy and saving computational time. The generated mesh is depicted in Figure 2.

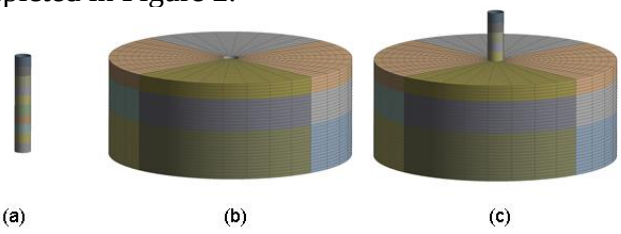

Figure 2. Mesh: **a** monopile, **b** soil, **c** assembly

2.4 *Loads and boundary conditions*

OWTs are exposed to more complex loading conditions than their onshore equivalents. The harsh marine environments together with specific design features cause complex loads which OWT monopiles have to withstand. According to DNV-OS-J101 standard (DNV, 2014), these loads can be categorised into eight groups, i.e. 1) aerodynamics loads; 2) wave loads; 3) current loads; 4) hydrostatic pressure loads; 5) inertia loads; 6) loads due to marine growth; 7) sea ice loads; 8) loads due to exceptional events (ship impact, earthquake etc.).

In this study, the aerodynamic, wave, current, hydrostatic pressure and inertia loads are considered. Other loads associated with marine growth, sea ice and exceptional events are not considered. These effects may play an important role for certain locations or more detailed investigation, but for the purpose of this study they are deemed negligible.

2.4.1 *Load cases*

In this study, both ultimate and fatigue load cases are considered. For the ultimate load case, the extreme sea condition (i.e. 50-year extreme wind condition combined with extreme wave and extreme current) represents a severe load and therefore is taken as a critical ultimate load case. For the fatigue load case, wind and wave fatigue loads for the normal operation of OWTs are considered. The current loads are not considered in the fatigue analysis, as the effect of current on the calculated stress range is relatively small and can be ignored in the fatigue analysis (GL, 2015).

Table 3 presents both extreme and normal sea condition considered in this study. The wind loads are presented in Table 4 and are taken from Ref. (LaNier, 2005) for WindPACT 3.6MW wind turbine, which is a reference wind turbine designed by NREL (National Renewable Energy Laboratory). Both current and wave loads on slender structural members, such as monopile submerged in water, can be calculated using Morrion's equation (DNV, 2014):

$$\begin{aligned} F &= F_d + F_m \\ &= \frac{1}{2}\rho_w C_d D|u_x|u_x + \rho_w C_m \frac{\pi D^2}{4} a_x \end{aligned} \quad (2)$$

where the first term is a drag force and the second term is an inertia force; ρ_w is the water density; C_d and C_m are the drag and inertia coefficient, respectively; D is the diameter of the cylinder; u_x and a_x are the horizontal wave-induced or current-induced velocity and acceleration of water, respectively.

It should be noted that the significant wave height, wave period, current speed in Table 3 and wind loads in Table 4 are to be modelled stochastically, and the details are presented in Section 3.

Table 3. Sea conditions (Kühn, 2001, Garcés García, 2012)

Item	Values	
	Extreme sea condition	Normal sea condition
Wind speed [m/s]	50	10
Significant wave height [m]	8.40	1.00
Wave period [s]	10.50	5.55
Current speed [m/s]	1.40	-

Table 4. Wind loads (LaNier, 2005)

Load case	Thrust [kN]	Bending moment [kN-m]
Ultimate	1,196	99,973
Fatigue	143	19,772

2.4.2 *Boundary conditions*

For the ultimate load case, the wind loads are applied to the monopile top, while both wave and current loads are applied to the monopile surface submerged into the water. The wind turbine weight on the top of the monopile is taken into account by applying a point load of 3,129 kN (LaNier, 2005) to the monopile top. Additionally, the hydrostatic pressure due to the sea water and the inertia loads due to the mass of monopile itself are also considered in this case, and these loads are automatically calculated by ANSYS software.

For the fatigue load case, the wind loads are applied to the monopile top, while the wave loads are applied to the monopile surface submerged into the water.

Additionally, for both loads cases, 1) the lateral boundaries of the soil model are fixed against lateral translation whereas the bottom of the soil model is fixed against translation in all directions; and 2) a frictional contact is defined between the contact surface of monopile and soil, enabling the soil-solid interaction.

3 IMPLEMENTATION OF STRUCTURAL RELIABILITY ASSESSMENT

In this section, the structural reliability of OWT monopiles is implemented, considering four limit states, i.e. ultimate, fatigue, deflection and buckling. The FEA model presented in Section 2 is used to perform stochastic FEA modelling of OWT monopiles, taking account of stochastic variables, such as wind loads, wave loads and soil properties. Regression is then used to post-process the results from FEA modelling to obtain the performance function expressed in terms of stochastic variables. After that, FORM is used to calculate the reliability index, obtaining reliability analysis results. The flowchart of the reliability analysis is presented in Figure 3.

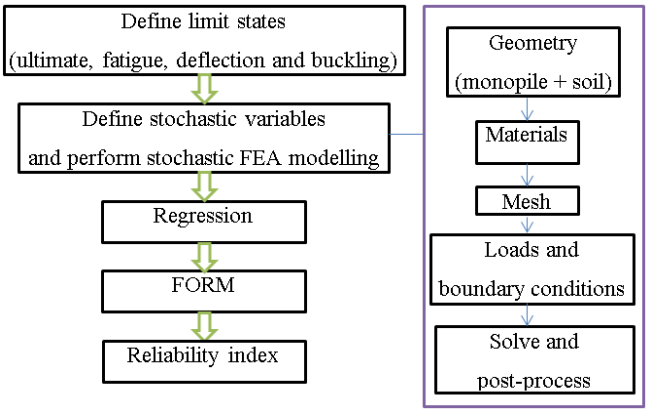

Figure 3. Flowchart of reliability analysis

3.1 *Ultimate limit state*

The ultimate limit state defines the ability of the structure to resist plastic collapse. For monopile structures, the equivalent stress is generally determined using the von-Mises stress theory. The limit state function for the von-Mises criterion can be expressed as:

$$g_u(x) = \sigma_{allow} - \sigma_{\max} \tag{3}$$

where subscript u denotes the ultimate limit state, σ_{allow} is the allowable stress, $\sigma_{\max}$ is the maximum von-Mises stress within monopile structure.

The allowable stress σ_{allow} in Eq. (3) can be expressed as:

$$\sigma_{allow} = \frac{\sigma_y}{\gamma_m} \tag{4}$$

where σ_y is the yield strength, with a value of 355MPa for Steel S355; γ_m is the material safety factor, with a value of 1.1 suggested by DNV-OS-J101 standard (DNV, 2014). Thus, the allowable stress σ_{allow} is 323 MPa.

3.2 *Fatigue limit state*

The fatigue limit state is particularly important in structures, such as OWT monopiles, subjected to significant cyclic loads. OWT monopiles normally have a long service period that may exceed 20 years. This, in conjunction with the inspection intervals, affects the reliability requirement of the monopile structural design.

According to the $S-N$ curve method, the number of loading cycles to failure, N, is given by:

$$\log N = A - m \log \Delta S \tag{5}$$

where A is the intercept; m is the slope of the $S-N$ curve in the log-log plot; ΔS is the stress range.

The intercept A and slope m in Eq. (5) are generally given by design standards, e.g. DNV-OS-J101 (DNV, 2014). In this study, the thickness-corrected cathodic-protected D curve given by DNV-OS-J101 (DNV, 2014) is chosen in the fatigue analysis.

The performance function of fatigue reliability analysis based on $S-N$ curve method is given by:

$$g_f = \log(N) - \log(N_t) \tag{6}$$

where subscript f denotes the fatigue limit state, N is the number of loading cycles to failure and can be obtained by using Eq. (5), N_t is the number of loading cycles expected during the given time period (e.g. 20 years).

3.3 *Deflection limit state*

Excessive deflections influence the serviceability of OWT monopiles and therefore should be avoided. The limit state function for deflection criteria can be expressed as:

$$g_d(x) = d_{allow} - d_{\max} \tag{7}$$

where subscript d denotes the deflection limit state, d_{allow} is the allowable deflection, and $d_{\max}$ is the maximum deflection.

Eq. 7 implies if the maximum deflection $d_{\max}$ exceeds the allowable deflection d_{allow}, failure occurs.

In this study, the allowable deflection d_{allow} in Eq. (7) is given by the following empirical equation suggested by DNV-OS-J101 standard (DNV, 2014):

$$d_{allow} = \frac{L}{200} \tag{8}$$

where L is the length of the monopile.

In this study, the monopile length L is 30m, and thus the allowable deflection d_{allow} is 0.15m.

3.4 *Buckling limit state*

OWT monopiles are generally thin-walled structure and can be prone to buckling failure. Therefore, buckling should be considered in the design of monopiles. The limit state function for buckling criterion can be expressed as:

$$g_b(x) = L_m - L_{m,\min} \tag{9}$$

where subscript b denotes the buckling limit state; L_m is the buckling load multiplier, which is the ratio of the critical buckling load to the applied load on the monopile structure; $L_{m\_\min}$ is the minimum allowable load multiplier.

Eq. 9 implies if the buckling load multiplier L_m less than the minimum allowable load multiplier $L_{m,\min}$, buckling failure occurs.

In this study, a value of 1.4 is chosen for the minimum allowable load multiplier $L_{m,\min}$, according to DNV standard (DNV, 2014).

3.5 *Stochastic variables and FEA*

The stochastic variables considered in this study are presented in Table 5. Eight stochastic variables are considered for ultimate load case. For fatigue load case, seven stochastic variables are considered, excluding the current speed. The COV of all stochastic variables are assumed to be 0.1. The mean values of these stochastic variables are given by Tables 2, 3 and 4.

Table 5. Stochastic variables for fatigue limit state

Variables	Descriptions	Distribution types (EN, 2002, DNV, 1992)	Load cases
x_1	Wind thrust	Normal	Fatigue and ultimate
x_2	Wind bending moment	Normal	Fatigue and ultimate
x_3	Significant wave height	Weibull	Fatigue and ultimate
x_4	Wave period	Lognormal	Fatigue and ultimate
x_5	Current speed	Weibull	Ultimate
x_6	Young's modulus of loose sand	Normal	Fatigue and ultimate
x_7	Young's modulus of medium clay	Normal	Fatigue and ultimate
x_8	Young's modulus of medium sand	Normal	Fatigue and ultimate

Having defined the stochastic variables, the FEA model presented in Section 2 is then used to perform stochastic FEA modelling of wind turbine monopile structures, with the help of the Design of Experiments module in ANSYS. It enables the input parameters being designated as stochastic parameters, having different types of distributions (such as normal, lognormal and Weibull distributions). A number of simulations have been

executed in ANSYS software, and the results are imported into a MATLAB code that has been developed for data regression, which is presented below.

3.6 *Regression*

Regression analysis is a statistical process for establishing relationship between a dependent variable and one or more independent variables. Taking the ultimate limit state as an example, the dependent variable (i.e. maximum von-Mises stress $\sigma_{\max}$) and independent variables (i.e. wind thrust x_1, wind bending moment x_2, significant wave height x_3, wave period x_4, current speed x_5, Young's modulus of loose sand x_6, Young's modulus of medium clay x_7, and Young's modulus of dense sand x_8) are assumed to have the following functional relationship:

$$\sigma_{\max} = [a_0, a_1, \cdots, a_{16}] \begin{bmatrix} 1 \\ x_1 \\ x_1^2 \\ \vdots \\ x_8 \\ x_8^2 \end{bmatrix} \tag{10}$$

$(a_0, a_1, \cdots, a_{16})$ in Eq. (10) are 17 regression coefficients. For other types of limit states, i.e. deflection, buckling and fatigue, expressions similar to Eq. 10 can be derived.

The regression coefficients for different limit states can be obtained using multivariate regression (Kolios, 2010).

Taking the maximum deflection as an example, the regression results are compared against the FEA results, as depicted in Figure 4. In this case, 300 stochastic FEA simulations are performed, obtaining 300 samples. The regression results presented in Figure 4 are calculated using the equation derived from multivarate regression. As can be seen from Figure 4, the regression results match well with the FEA results. The R square in this case is 0.99, which is relatively high and indicates the success of the multivariate regression used in this study.

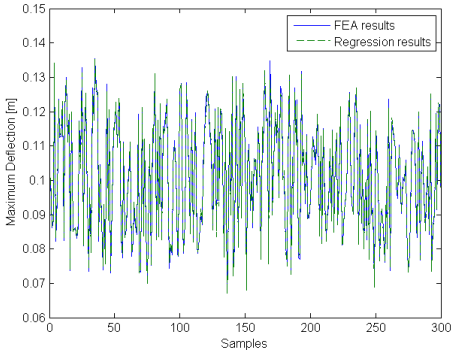

Figure 4. Comparison of FEA and regression results

3.7 *FORM (First Order Reliability Method)*

Having obtained the performance function from regression, the FORM (Hasofer and Lind, 1974) is used to calculate the reliability index β. The flowchart of FORM is summarised below.

1) Define the performance function for different limit state. Taking ultimate limit state as an example, substituting Eq. (10) into Eq. (3) yields the following performance function:

$$g_u(x) = \sigma_{allow} - [a_0, a_1, \cdots, a_{16}] \begin{bmatrix} 1 \\ x_1 \\ x_1^2 \\ \vdots \\ x_8 \\ x_8^2 \end{bmatrix} \tag{11}$$

2) Set the mean value point as an initial design point, i.e. $x_{i,k} = \mu_{x_i}$ $i = 1,2,\cdots,n$, and calculate the gradients $\nabla g(X_k)$ of the limit-state function at this design point. Here, $x_{i,k}$ refers to the i^{th} element in the vector X_k of the k^{th} iteration, and μ_{x_i} is the mean value of the i^{th} element;

3) Calculate the initial reliability index β using the mean-value method, i.e. $\beta = \mu_{\tilde{g}} / \sigma_{\tilde{g}}$ and its direction cosine α.

$$\beta = \mu_{\tilde{g}} / \sigma_{\tilde{g}} = \frac{g(\mu_X)}{\left[\sum_{i=1}^{n} \left(\frac{\partial g(\mu_X)}{\partial x_i}\right)^2 \sigma_{x_i}^2\right]^{1/2}} \tag{12}$$

$$\alpha_i = -\frac{\frac{\partial g(X^*)}{\partial x_i}\sigma_{x_i}}{\left[\sum_{i=1}^{n} \left(\frac{\partial g(X^*)}{\partial x_i}\sigma_{x_i}\right)^2\right]^{1/2}} \tag{13}$$

4) Compute a new design point X_k and U_k, function value, and gradients at this new design point.

$$x_{i,k} = \mu_{x_i} + \beta\sigma_{x_i}\alpha_i \tag{14}$$

$$u_{i,k} = \frac{x_{i,k} - \mu_{x_i}}{\sigma_{x_i}} \tag{15}$$

5) Compute the reliability index β and direction cosine α using Eqs. (14) and (15), respectively.

$$\beta = \frac{g(U^*) - \sum_{i=1}^{n} \frac{\partial g(U)}{\partial x_i}\sigma_{x_i} u_i^*}{\sqrt{\sum_{i=1}^{n}\left(\frac{\partial g(U^*)}{\partial x_i}\sigma_{x_i}\right)^2}} \tag{16}$$

$$\alpha_i = -\frac{\frac{\partial g(X^*)}{\partial x_i}\sigma_{x_i}}{\left[\sum_{i=1}^{n}\left(\frac{\partial g(X^*)}{\partial x_i}\sigma_{x_i}\right)^2\right]^{1/2}} \tag{17}$$

6) Repeat Steps 4) to 5) until the convergence of reliability index β.

A Matlab code was developed in this study to calculate the reliability index β using FORM based on the above flowchart.

4 RESULTS AND DISCUSSION

Table 6 summarises the limit states that have been considered in the reliability assessment of OWT monopiles. A short description and the corresponding equation of each limit state are also included in Table 6.

Table 6. Summary of limit states

Limit states	Descriptions	Equations
g_u	Ultimate limit state	Eq. 3
g_f	Fatigue limit state	Eq. 6
g_d	Deflection limit state	Eq. 7
g_b	Buckling limit state	Eq. 9

Table 7 presents the reliability index β obtained from reliability analysis of each limit state. The overall value of the reliability index β is then derived as the minimum value calculated from each of the limit states examined.

Table 7. Reliability index of monopile structure

Item	Value	Description
β_u	8.903	Ultimate limit state
β_f	1.106	Fatigue limit state
β_d	4.035	Deflection limit state
β_b	8.883	Buckling limit sate
β	1.106	Overall

As can be seen from Table 7, the fatigue limit state dominates the design of wind turbine monopiles, as fatigue reliability index β_f is much smaller than other reliability index.

In terms of fatigue reliability, we can also predict the reliability index over time. Figure 5 presents the reliability index over 20-year service time. As can be seen from Figure 5, the reliability index reduces with time, reaching the lowest value of 1.106 in Year 20.

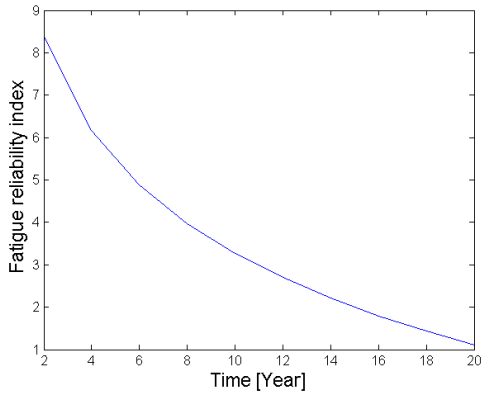

Figure 5. Fatigue reliability index over 20-year service life

Additionally, a case study is performed to investigate the effects of COV of stochastic variables on the fatigue reliability index. In this case, three values of COV are considered, i.e. 0.08, 0.10 and 0.12. The calculated fatigue reliability index over 20-year service life with different values of COV is depicted in Figure 6. As can be seen from Figure 6, the reliability index is sensitive to the value of COV. The higher value of COV means higher uncertainties in stochastic variables, resulting in lower reliability.

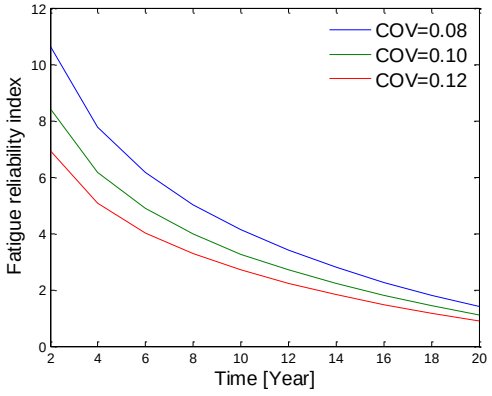

Figure 6. Fatigue reliability index with different COV

5 CONCLUSIONS

In this work, a generic framework for reliability assessment of OWT (offshore wind turbine) monopiles is developed. The framework starts with defining limit state. Four types of limit states are considered, i.e. ultimate, fatigue, deflection and buckling. A 3D (three-dimensional) parametric FEA (finite element analysis) model of OWT monopiles is developed, taking account of soil-solid interaction and stochastic variables (i.e. soil properties, wind, wave and current loads). With the help of multivariate regression, the results from the stochastic FEA simulations are used to derive the performance function expressed in terms of stochastic variables. After that, FORM (first order reliability method) is used to calculate the reliability index. The proposed framework is applied to reliability assessment of a 30m-length monopile. The results show that 1) the fatigue reliability is dominant in the design; 2) the reliability index is sensitive to the values of COV (coefficient of variation); and 3) the higher value of COV means higher uncertainties in stochastic variables, resulting in lower reliability. The proposed framework is generic in nature and capable of effectively assessing reliability of OWT monopiles, providing the possibility to optimise the OWT monopiles to meet target reliability.

REFERENCES

ABDEL-RAHMAN, K. & ACHMUS, M. Finite element modelling of horizontally loaded monopile foundations for offshore wind energy converters in Germany. Proceedings of the international symposium on frontiers in offshore geotechnics. Taylor and Francis, Perth, 2005. 391-396.

BRADY, N. C. & WEIL, R. R. 1996. *The nature and properties of soils*, Prentice-Hall Inc.

COUNCIL, G. W. E. 2016. Global wind statistics 2015. *Report. Brussels, Belgium: GWEC*.

DNV 1992. *Structural reliability analysis of marine structures*, Det Norske Veritas.

DNV 2014. DNV-OS-J101: Offshore standard for design of offshore wind turbine structures.

DRUCKER, D. C. & PRAGER, W. 1952. Soil mechanics and plastic analysis or limit design. *Quarterly of applied mathematics*, 10**,** 157-165.

EN, B. 2002. BS EN 1990 (2002): Eurocode - Basis of structural design.

EWEA 2015. Offshore Wind in Europe - Walking the tightrope to success. European Wind Energy Association.

EWEA 2016. Wind in power - 2015 European statistics. European Wind Energy Association

GARCÉS GARCÍA, C. 2012. Design and calculus of the foundation structure of an offshore monopile wind turbine.

GEOTECHDATA. 2016. *http://www.geotechdata.info/; accessed at 22-06-2016.* [Online].

GL, D. 2015. DNVGL-RP-C210: Probabilistic methods for planning of inspection for fatigue cracks in offshore structures.

GL, D. 2016. DNVGL-ST-0126: Support structures for wind turbines.

HASOFER, A. M. & LIND, N. C. 1974. Exact and invariant second-moment code format(for reliability analysis in multivariate problems). *American Society of Civil Engineers, Engineering Mechanics Division, Journal*, 100**,** 111-121.

JUNG, S., KIM, S.-R. & PATIL, A. 2015. Effect of monopile foundation modeling on the structural response of a 5-MW offshore wind turbine tower. *Ocean Engineering*, 109**,** 479-488.

KOLIOS, A. I. 2010. A multi-configuration approach to reliability based structural integrity assessment for ultimate strength.

KÜHN, M. J. 2001. *Dynamics and design optimisation of offshore wind energy conversion systems*, TU Delft, Delft University of Technology.

LANIER, M. W. 2005. LWST Phase I project conceptual design study: Evaluation of design and construction approaches for economical hybrid steel/concrete wind turbine towers; June 28, 2002--July 31, 2004. National Renewable Energy Lab., Golden, CO (US).

PETRINI, F., MANENTI, S., GKOUMAS, K. & BONTEMPI, F. 2010. Structural design and analysis of offshore wind turbines from a system point of view. *Wind Engineering*, 34**,** 85-108.

SM, D. R. 2000. Recommended Practice for Planning, Designing and Constructing Fixed Offshore Platforms—Working Stress Design.

WANG, L., KOLIOS, A., DELAFIN, P.-L., NISHINO, T. & BIRD, T. 2015. Fluid Structure Interaction Modelling of A Novel 10MW Vertical-Axis Wind Turbine Rotor Based on Computational Fluid Dynamics and Finite Element Analysis. *EWEA 2015 Annual Event, France, Paris*.

WANG, L., KOLIOS, A., NISHINO, T., DELAFIN, P.-L. & BIRD, T. 2016a. Structural optimisation of vertical-axis wind turbine composite blades based on finite element analysis and genetic algorithm. *Composite Structures*.

WANG, L., LIU, X. & KOLIOS, A. 2016b. State of the art in the aeroelasticity of wind turbine blades: Aeroelastic modelling. *Renewable and Sustainable Energy Reviews*, 64**,** 195-210.

WANG, L., LIU, X., RENEVIER, N., STABLES, M. & HALL, G. M. 2014. Nonlinear aeroelastic modelling for wind turbine blades based on blade element momentum theory and geometrically exact beam theory. *Energy*, 76**,** 487-501.

WANG, L., QUANT, R. & KOLIOS, A. 2016c. Fluid structure interaction modelling of horizontal-axis wind turbine blades based on CFD and FEA. *Journal of Wind Engineering and Industrial Aerodynamics*, 158**,** 11-25.

WILKES, J., MOCCIA, J., ARAPOGIANNI, A., DRAGAN, M., PLYTAS, N., GENACHTE, A., GUILLET, J. & WILCZEK, P. 2016. The European offshore wind industry key 2015 trends and statistics. *European Wind Energy Association*.